HYDROGEN, FUEL CELL & ENERGY STORAGE

The Effect of Using an ETC Collector on Increasing the Geothermal Fluid Temperature in a Multigeneration System

Eman Shakir Hussein Hussein | Iraj Mirzaee*

Samrand Rash-Ahmadi | Morteza Khalilian

Mechanical Engineering Department, Engineering Faculty, Urmia University, Urmia, Iran

* Corresponding author, Email: i.mirzaee@urmia.ac.ir

Article Information

Article Type
Research Article

Article History
Received: *11 Oct 2025*
Revised: *15 Nov 2025*
Accepted: *20 Dec 2025*
Published Online: *05 Jan 2026*

Keywords

ETC collector
Geothermal energy
Multigeneration system
Working fluids
Thermodynamic analysis

Abstract

The research presents a new power generation system which combines geothermal power with solar capabilities, providing a sustainable and efficient energy production solution. The system relies on an evacuated tube collector (ETC) to heat geothermal fluid before it is used in various subsystems. Raising the temperature is crucial for enhancing the operational efficiency of various subsystems within the system. The multigeneration setup consists of five coordinated units, including an ORC electricity generator that produces power while also supplying energy for two subsystems: double-effect absorption cooling and domestic thermal heating to meet energy demand. The integrated system operates PEM electrolyzers alongside hydrogen production and operates reverse osmosis units to generate freshwater through desalination process. The study results indicate that increasing the solar energy received by the collector significantly enhances the overall system performance. As solar energy increases, both the power output and the collector outlet temperature improve. The system's performance efficiency directly depends on outlet collector temperature, which affects both hydrogen and freshwater production rates. Raising the solar radiation intensity makes the ETC produce more energy and exergy, leading to enhanced overall system operation. Among the tested working fluids, R600 exhibits the best performance, producing 55.16 kg/day of hydrogen and delivering 1.451 kg/s of freshwater – outperforming other fluids in both categories.

Cite this article: Hussein, E. S. H., Mirzaee, I., Rash-Ahmadi, S., Khalilian, M. (2026). The Effect of Using an ETC Collector on Increasing the Geothermal Fluid Temperature in a Multigeneration System. DOI: 10.22104/hfe.2025.7456.1346

 Publisher: Iranian Research Organization for Science and Technology (IROST)
DOI: 10.22104/hfe.2025.7456.1346

1 Introduction

The method of providing energy has emerged as a significant global issue today. The heavy reliance of industrialized nations on fossil fuels and their overconsumption not only depletes vast underground reserves accumulated over centuries but also leads to severe environmental pollution. The growing energy demand, limited fossil fuel reserves, and their harmful environmental consequences – particularly global warming – have accelerated the shift toward clean energy sources [1]. Energy sources can be categorized into three types: traditional fossil fuels, nuclear power, and renewable energies, with the latter – such as solar and geothermal – distinguished by their capacity for natural replenishment. The primary motivations for shifting towards renewable energy lies in its potential to mitigate environmental issues. Emissions of pollutants such as carbon monoxide, nitrogen oxides, and greenhouse gases are major contributors to air pollution and global warming – problems increasingly recognized as serious global threats. In recent years, industrial development has significantly increased the release of these harmful emissions [2].

Undeniably, renewable energies are crucial for the future of global energy systems. Unlike nuclear technologies, which pose challenges such as radioactive waste management, renewables are technologically simpler and more environmentally sustainable. Future energy systems must undergo fundamental and structural reforms, prioritizing the use of carbon-free sources – such as wind, solar, and geothermal energy – alongside carbon-neutral alternatives like biomass. Furthermore, to maximize the effective use of naturally available energy sources, researchers have been exploring traditional energy production technologies and replacing them with advanced, high-efficiency systems. Among these, cogeneration systems have emerged as a promising solution to address the identified challenges [3]. In recent years, cogeneration systems have been increasingly adopted across various consumer sectors, maximizing the efficiency of primary fuel use and demonstrating high operational effectiveness. This not only reduces environmental impact but also contributes to the conservation of fuel resources [4]. It is noteworthy that when cogeneration systems are combined with renewable energy sources like solar power, they can serve as effective alternatives to conventional systems, offering a clean and cost-effective solution. Recently, a plethora of studies has been undertaken in the area of multigeneration systems utilizing renewable energy sources.

Mokhtari and Haqiqati [5] investigated an Organic Rankine Cycle (ORC) system designed for electricity generation, utilizing ground source heat combined with flat plate collectors (FPC) as the primary sources of thermal energy. For energy tank, a hydrogen system consisting of a fuel cell and a proton electrolyte membrane (PEM) electrolyzer was utilized. The results revealed that the evaluated cycle has a payback period of 6.32 years and a levelized cost of electricity (LCOE) of $0.26 per kWh. Additionally, from an environmental standpoint, the system is expected to decrease CO_2 emissions by 583.3 tons annually. Forghani et al. [6] examined a multigeneration cycle that combines solar and geothermal energy to meet the needs for fresh water, heating, cooling, and electricity. Their design utilized geothermal wells, flat plate collectors (FPC), and photovoltaic (PV) panels to supply the necessary heat and power. The research indicated that the objective function improved by 14.38%, 54.61%, and 59.78% when solar energy, geothermal energy, and a hybrid of both were utilized, respectively, compared to the baseline scenario.

Ren et al. [7] enhanced a combined cooling, heating, and power (CCHP) system by integrating solar electricity, geothermal energy, and solar thermal energy to meet the energy demands of three different types of buildings. Their findings indicated that the electrical load tracking approach outperformed other control strategies in terms of effectiveness. Furthermore, Alirahmi et al. [8] investigated Combined Cooling, Heating, and Power (CCHP) systems integrated with parabolic solar collectors and geothermal energy for hydrogen production, aiming to improve overall system efficiency. Their results showed that at the optimal operating point, the system achieved a total unit cost of 129.7 $/GJ and an exergy efficiency of 29.95%.

Additionally, Zarei et al. [9] optimized a hybrid solar Combined Cooling, Heating, and Power (CCHP) system, revealing that the incorporation of booster compressors into the cooling subsystem significantly improves overall system performance. Their findings indicated that the integration of a booster compressor significantly improves system effectiveness, demonstrating a 96.34% increase in the coefficient of performance (COP), a 55.1% boost in exergy efficiency, and a 121.9% rise in net output power. Additionally, the improved system contributed to environmental sustainability by preventing the emission of 2,504 kg of carbon dioxide annually. Calise et al. [10] evaluated the performance of two hybrid systems that integrated either evacuated flat-plate solar collectors or photovoltaic (PV) technology with geothermal energy. For comparison purposes, the systems were assessed based on their ability to generate electricity as well as provide heating and cooling. The systems were comprised of ORC,

ARC, a biomass auxiliary heater, along with electric and thermal storage systems to accommodate variations in the solar system. The photovoltaic (PV) system exhibited a shorter payback period compared to the evacuated flat plate collectors. Yilmaz and Sen [11] conducted a comprehensive study on the feasibility of energy consumption and costs for a combined solar and geothermal multigeneration plant. Their analysis identified optimal exergy and energy efficiencies of 43.5% and 19.5%, respectively.

Based on the review of previous studies and the identified research gaps, the main originality of this study lies in the integration of an Evacuated Tube Solar Collector (ETSC) into the system design – a component that has received limited attention in earlier research. This paper investigates Thermoelectric Generators (TEGs) as an innovative power generation method which operates without requiring traditional energy supply systems. It also distinguishes itself by focusing on double-effect absorption chillers, a component that has been underrepresented in existing research, in contrast to the extensive attention given to single-effect absorption chillers in the literature.

2 System Description

The proposed system, illustrated in Figure 1, comprises a low-grade geothermal resource, EVTSCs, an ORC cycle, a reverse osmosis system, a double-effect absorption refrigeration system and a proton exchange membrane electrolyzer. This cycle aims to generate heat, electricity, freshwater, cooling, and hydrogen. The temperature of the low-grade geothermal fluid is elevated by the ETSC when exposed to solar radiation.

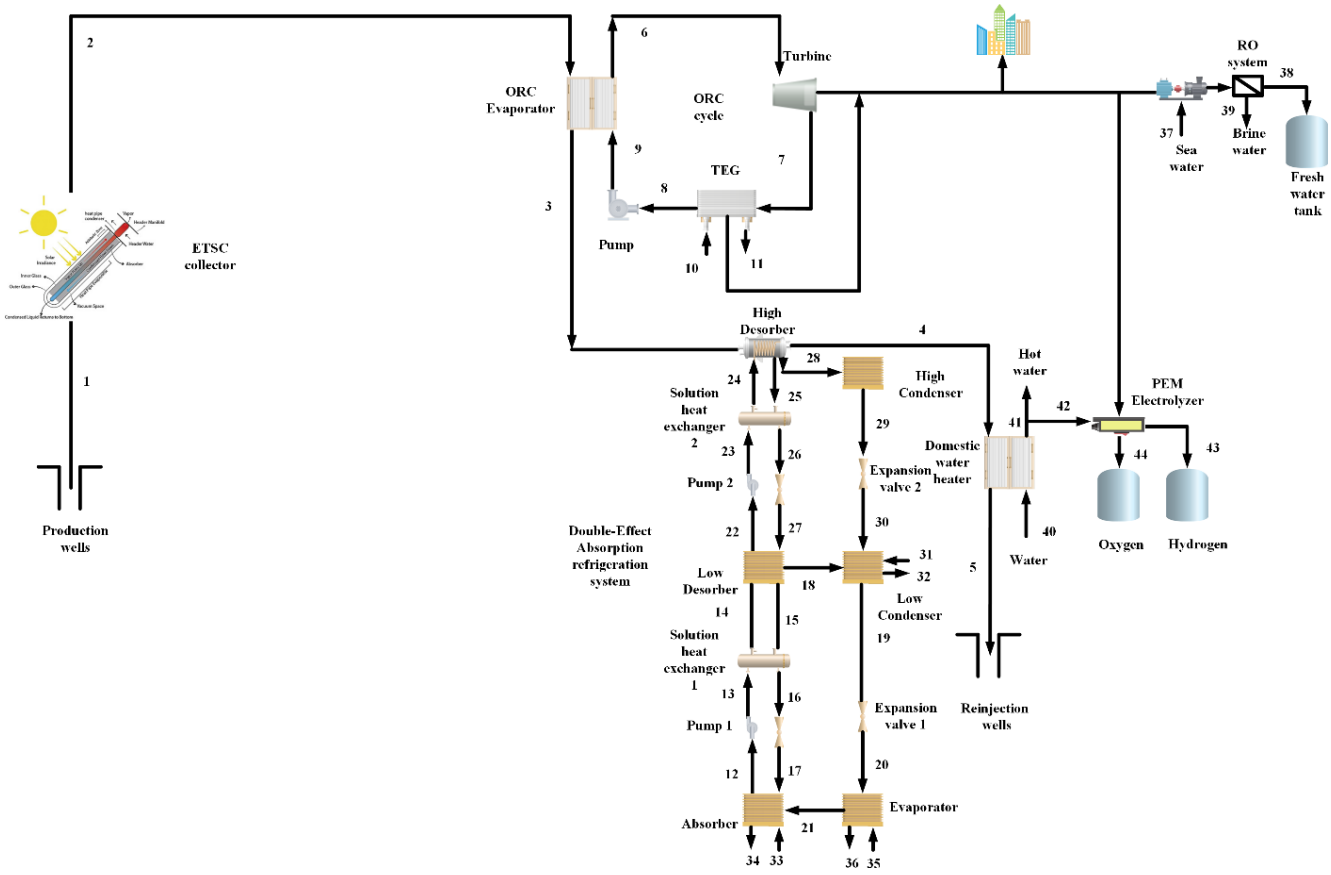

Fig. 1. The multigeneration system suggested in this study.

The hot geothermal fluid is first directed to the ORC evaporator where it serves as the heat source for the steam cycle. At point 2, the working fluid absorbs thermal energy from the geothermal steam via a steam generator, producing vapor to drive the turbine. The hot water exiting the steam generator at point 3 retains residual thermal energy, which is subsequently utilized to operate the generator of a double-

effect absorption cooling system. Following this stage, the produced steam is used to preheat the feed water for a PEM electrolyzer at point 40 through a domestic water heater (DWH). The geothermal fluid is finally channeled into the reinjection well. Simultaneously, the electricity generated by the ORC cycle and TEG unit supplies power to a reverse osmosis desalination system and the PEM electrolyzer, enabling the production of both freshwater and hydrogen for various applications.

Thermodynamic analysis relies on specific assumptions. The assumptions made regarding the system in question are as follows:

- Geothermal hot water is presumed to be clean and free from contaminants.
- It is presumed that all turbines, pumps, condensers, and valves function as adiabatic systems.
- Heat loss from the system boundaries is considered negligible.
- The system functions under steady-state conditions.
- Variations in potential and kinetic energy, along with pressure reductions in pipes and heat exchangers, are disregarded.
- The outlet from the absorber and both outlets from the desorber are assumed to be in equilibrium.
- It is assumed that solar radiation is consistent and uniform.

The necessary equations to model the system are introduced as follows:

$$\sum \dot{m}_{\text{in}} - \sum \dot{m}_{\text{out}} = \frac{dm_{\text{cv}}}{dt}\,, \tag{1}$$

$$\dot{Q} - \dot{W} + \sum_{\text{in}} \dot{m}_{\text{in}}\left(h_{\text{in}} + \frac{V_{\text{in}}^2}{2} + gZ_{\text{in}}\right) - \sum_{\text{out}} \dot{m}_{\text{out}}\left(h_{\text{out}} + \frac{V_{\text{out}}^2}{2} + gZ_{\text{out}}\right) = \frac{dE_{\text{cv}}}{dt}\,, \tag{2}$$

$$\dot{\text{Ex}}_Q + \sum_{\text{in}} \dot{m}_{\text{in}}\text{ex}_{\text{in}} = \sum_{\text{out}} \dot{m}_{\text{out}}\text{ex}_{\text{out}} + \dot{\text{Ex}}_W + \dot{\text{Ex}}_D\,, \tag{3}$$

m and $\dot{m}$ represent mass and mass flow rate. In this regard, in and out indices represent the inlet and outlet of the volume control. Moreover, $\dot{W}$, $\dot{Q}$, E and t display the work rate, heat transfer rate, energy and time. Moreover, h, v, g and Z represent enthalpy, speed, gravitational acceleration and height, respectively. Furthermore, $\dot{\text{Ex}}_D$ is the exergy destruction rate, $\dot{\text{Ex}}_Q$ is the exergy rate of heat, $\dot{\text{Ex}}_W$ is the exergy rate of work and ex is the specific exergy.

The equations used to model the solar collector are:

The ETCs efficiency can be expressed as [12]:

$$\eta_{\text{ETC}} = 0.536 - \frac{0.824(T_{\text{ETC}} - T_0)}{G_b} - \frac{0.0069(T_{\text{ETC}} - T_0)^2}{G_b}\,, \tag{4}$$

$$T_{\text{ETC}} = \frac{T_{\text{in}} + T_{\text{out}}}{2}\,, \tag{5}$$

in which T_{ETC} is the mean temperature of the ETC collector. The amount of the heat absorbed by the ETC collector is expressed as:

$$Q_{\text{ETC}} = N_{\text{ETC}}\,\eta_{\text{ETC}}\,G_b\,A_{\text{ETC}} = c_p m_E(T_{\text{in}} - T_{\text{out}}) \tag{6}$$

where N_{ETC} is the number of the ETC modules, A_{ETC} is the area of ETCs m_E is the water mass flow rate of the ETC.

The energy and power transferred, along with the rate of exergy loss for each component in the suggested multigeneration system, can be assessed using the energy and exergy balance equations listed in Table 1.

3 Results and Discussion

In this research, the temperature of the geothermal resource fluid is enhanced by integrating an Evacuated Tube Collector (ETC) with a surface area of 140 m^2. This system supports multiple outputs, including power generation, freshwater production, freshwater heating, and hydrogen generation. A key outcome of this setup is the elevation of the outlet water temperature from the ETC collector, which is achieved by harnessing solar energy. Figure 2 illustrates the variations in the exit water temperature of the ETC based on the solar radiation received by the collector. The system is analyzed for varying total energy outputs from the ETC collector, ranging from 30 kW to 90 kW. The results show that the temperature of the geothermal resource (initially at 360 K) increases to 401.1 K and 436.8 K as the energy output from the ETC collector rises from 30 kW to 90 kW, respectively. It is evident that a rise in energy generated by the solar collector positively impacts the collector's outlet temperature.

Figure 3 illustrates the distribution of energy and exergy from the solar radiation that strikes the ETC collector, with solar radiation ranging between 300 and 900 W/m^2. At a solar radiation intensity of 900 W/m^2, the total energy and exergy are calculated to be 127.4 kW and 92.5 kW, respectively. Conversely, at solar radiation at 300 W/m^2, the calculated total energy and exergy are 42 kW and 32.2 kW, respectively. It is evident that the exergy is lower than the energy due to exergy losses caused by increased entropy, which reduces the useful work that can be extracted from the energy.

Figure 4 illustrates the impact of the total energy output from the solar collector on the power output in the ORC cycle and the overall system. As previously mentioned, the solar collector increases the temperature of the geothermal fluid and provides the essential energy required for the subsystem. The graphs demonstrate that as the generated energy increases from 30 kW to 90 kW, both the power output from the ORC system and the overall system's power generation also rise. Specifically, when the solar collector's energy production increases from 30 kW to 90 kW, the power output from the ORC cycle grows from 56.29 kW to 67.38 kW, while the total power generation rate increases from 35.87 kW to 86.31 kW. The overall power generation is influenced by the net power produced in the ORC cycle and the TEG unit's contribution.

Figure 5 demonstrates the effect of the collector outlet temperature on the hydrogen and freshwater production rates. The results indicate that as the outlet temperature of the collector increases, both the hydrogen and freshwater production rates rise. This rise can be explained by the reality that elevated outlet temperatures facilitate more energy transfer to the ORC cycle, thereby improving the production rates of both hydrogen and freshwater. It is clear that as the collector outlet temperature rises from 430 K to 530 K, the hydrogen production rate increases from 17.19 kg/day to 43.28 kg/day, and the hydrogen production rate goes up from 0.8084 kg/s to 1.285 kg/s. This demonstrates that a 23.2% increase in temperature leads to a 151.7% surge in hydrogen production and a 58.9% increase in freshwater production.

Table 1. Energy balance equations and exergy destruction rates for every element of the suggested system.

Parts	equations of energy balance	equations of exergy destruction rate
Solar collector	$\dot{m}_1 h_1 + \dot{Q}_u = \dot{m}_2 h_2$	$\dot{E}x_{D,\mathrm{col}} = \dot{E}x_{\mathrm{sun}} + \dot{E}x_1 - \dot{E}x_2$
ORC evaporator	$\dot{Q}_{\mathrm{eva,ORC}} = \dot{m}_2(h_2 - h_3) = \dot{m}_6(h_6 - h_9)$	$\dot{E}x_{D,\mathrm{eva,ORC}} = \dot{E}x_2 + \dot{E}x_9 - \dot{E}x_3 - \dot{E}x_6$
ORC turbine	$\dot{W}_{t,\mathrm{ORC}} = \dot{m}_6(h_6 - h_7)$	$\dot{E}x_{D,t,\mathrm{ORC}} = \dot{E}x_6 - \dot{W}_{t,\mathrm{ORC}} - \dot{E}x_7$
ORC TEG	$\dot{Q}_{\mathrm{TEG,ORC}} = \dot{m}_7(h_7 - h_8) = \dot{m}_{10}(h_{11} - h_{10})$	$\dot{E}x_{D,\mathrm{TEG,ORC}} = \dot{E}x_7 + \dot{E}x_{10} - \dot{E}x_8 - \dot{E}x_{11}$
ORC pump	$\dot{W}_{p,\mathrm{ORC}} = \dot{m}_8(h_9 - h_8)$	$\dot{E}x_{D,p,\mathrm{ORC}} = \dot{W}_{p,\mathrm{ORC}} - \dot{E}x_8 + \dot{E}x_9$
DEARC-High desorber	$\dot{Q}_{\mathrm{Hdes,DEARC}} = \dot{m}_3(h_3 - h_4)$	$\dot{E}x_{d,\mathrm{DEARC,Hdes}} = \dot{E}x_3 + \dot{E}x_{24} - \dot{E}x_4 - \dot{E}x_{25} - \dot{E}x_{28}$
DEARC-High condenser	$\dot{Q}_{\mathrm{Hcond,DEARC}} = \dot{m}_{28}(h_{28} - h_{29})$	$\dot{E}x_{d,\mathrm{Hcond,DEARC}} = \dot{E}x_{28} - \dot{E}x_{29}$
DEARC-Solution heat exchanger 1	$\dot{Q}_{\mathrm{SHX1,DEARC}} = \dot{m}_{15}(h_{15} - h_{16}) = \dot{m}_{13}(h_{14} - h_{13})$	$\dot{E}x_{d,\mathrm{SHX1,DEARC}} = \dot{E}x_{13} + \dot{E}x_{15} - \dot{E}x_{14} - \dot{E}x_{16}$
DEARC-Solution heat exchanger 2	$\dot{Q}_{\mathrm{SHX2,DEARC}} = \dot{m}_{25}(h_{25} - h_{26}) = \dot{m}_{23}(h_{24} - h_{23})$	$\dot{E}x_{d,\mathrm{SHX2,DEARC}} = \dot{E}x_{23} + \dot{E}x_{25} - \dot{E}x_{24} - \dot{E}x_{26}$
DEARC-Low condenser	$\dot{Q}_{\mathrm{Lcond,DEARC}} = \dot{m}_{18}h_{18} + \dot{m}_{30}h_{30} - \dot{m}_{19}h_{19} = \dot{m}_{31}(h_{32} - h_{31})$	$\dot{E}x_{d,\mathrm{Lcond,DEARC}} = \dot{E}x_{18} + \dot{E}x_{30} + \dot{E}x_{31} - \dot{E}x_{19} - \dot{E}x_{32}$
DEARC-Evaporator	$\dot{Q}_{\mathrm{eva,DEARC}} = \dot{m}_{21}(h_{21} - h_{20}) = \dot{m}_{35}(h_{36} - h_{35})$	$\dot{E}x_{d,\mathrm{eva,DEARC}} = \dot{E}x_{20} + \dot{E}x_{35} - \dot{E}x_{21} - \dot{E}x_{36}$
DEARC-Absorber	$\dot{Q}_{\mathrm{Abs,DEARC}} = \dot{m}_{21}h_{21} + \dot{m}_{17}h_{17} - \dot{m}_{12}h_{12} = \dot{m}_{33}(h_{34} - h_{33})$	$\dot{E}x_{d,\mathrm{Abs,DEARC}} = \dot{E}x_{21} + \dot{E}x_{17} + \dot{E}x_{33} - \dot{E}x_{12} - \dot{E}x_{34}$
DEARC-Pump 1	$\dot{W}_{p1,\mathrm{DEARC}} = \dot{m}_{12}(h_{13} - h_{12})$	$\dot{E}x_{d,p1,\mathrm{DEARC}} = \dot{W}_{p1,\mathrm{DEARC}} + \dot{E}x_{12} - \dot{E}x_{13}$
DEARC-Pump 2	$\dot{W}_{p2,\mathrm{DEARC}} = \dot{m}_{22}(h_{23} - h_{22})$	$\dot{E}x_{d,p2,\mathrm{DEARC}} = \dot{W}_{p2,\mathrm{DEARC}} + \dot{E}x_{22} - \dot{E}x_{23}$
PEM	$\dot{W}_{\mathrm{PEM}} = \dot{m}_{42}h_{42} - \dot{m}_{43}h_{43} - \dot{m}_{44}h_{44}$	$\dot{E}x_{D,\mathrm{PEM}} = \dot{E}x_{42} + \dot{W}_{\mathrm{PEM}} - \dot{E}x_{43} - \dot{E}x_{44}$
DWH	$\dot{Q}_{\mathrm{DWH}} = \dot{m}_4(h_4 - h_5) = \dot{m}_{40}(h_{41} - h_{40})$	$\dot{E}x_{\mathrm{DWH}} = \dot{E}x_4 + \dot{E}x_{40} - \dot{E}x_5 - \dot{E}x_{41}$
RO	$\dot{W}_{\mathrm{RO}} = \dot{m}_{37}h_{37} - \dot{m}_{38}h_{38} - \dot{m}_{39}h_{39}$	$\dot{E}x_{D,\mathrm{RO}} = \dot{E}x_{37} - \dot{E}x_{38} - \dot{E}x_{39}$
COP	$\mathrm{COP} = \dfrac{\dot{Q}_{\mathrm{eva,DEARC}}}{\dot{Q}_{\mathrm{Hdes,DEARC}} + \dot{W}_{\mathrm{net,DEARC}}}$	
Thermal efficiency	$\eta_{\mathrm{th,tot}} = \dfrac{\dot{W}_{\mathrm{ORC}}\dot{W}_{\mathrm{TEG}} + \dot{Q}_{\mathrm{cooling}} + \dot{Q}_{\mathrm{DWH}} + \dot{m}_{43}\mathrm{HHV}_{\mathrm{H_2}} - \dot{W}_{\mathrm{PEM}} + \dot{m}_{38}h_{38} - \dot{W}_{\mathrm{RO}}}{\dot{Q}_u + \dot{m}_1 h_1}$	
Exergy efficiency	$\eta_{\mathrm{ex,tot}} = \dfrac{\dot{W}_{\mathrm{ORC}} + \dot{W}_{\mathrm{TEG}} + \dot{E}x_{\mathrm{cooling}} + \dot{E}x_{43}\dot{E}x_{44} + \dot{E}x_{41} - \dot{E}x_{40} + \dot{E}x_{38}}{\dot{E}x_{\mathrm{in,sun}} + \dot{E}x_1}$	

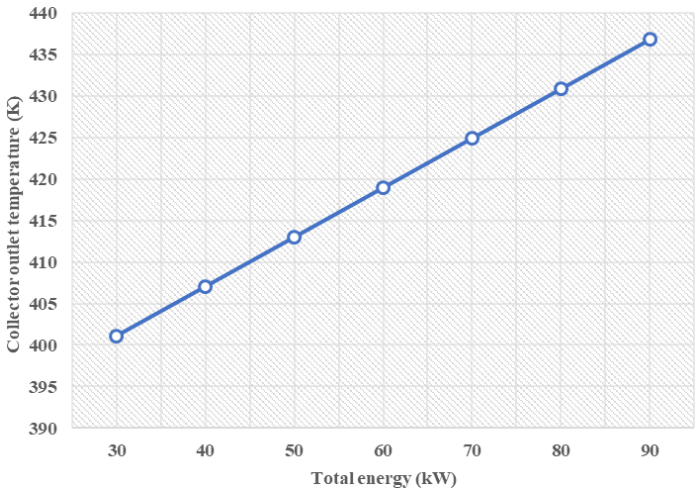

Fig. 2. The influence of the solar collector's total energy on the temperature at the collector outlet.

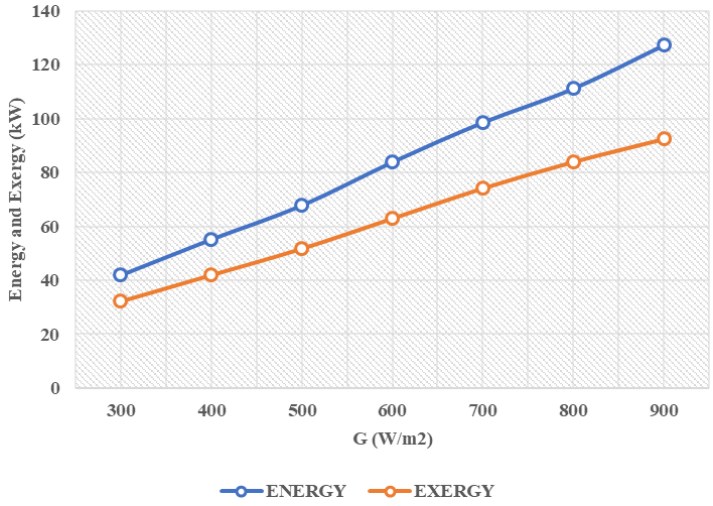

Fig. 3. The effect of solar intensity on the distribution of energy and exergy.

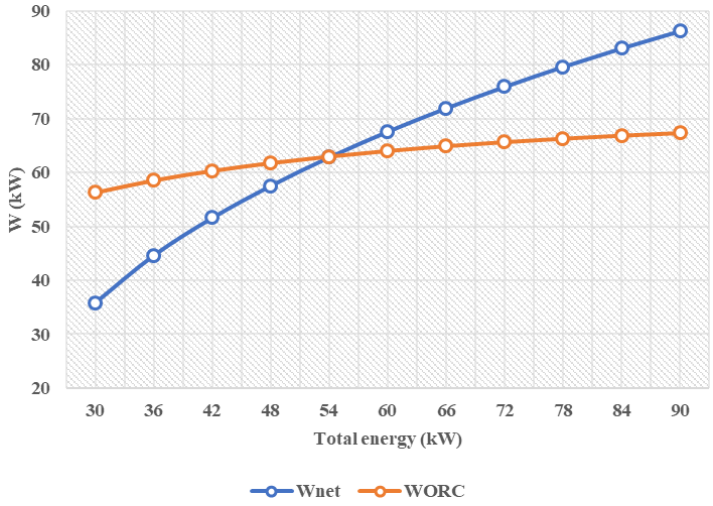

Fig. 4. The impact of the overall energy from the solar collector on the power output generated in the ORC cycle and the entire system.

Figure 6 compares five different working fluids used in the ORC cycle with respect to hydrogen and fresh-

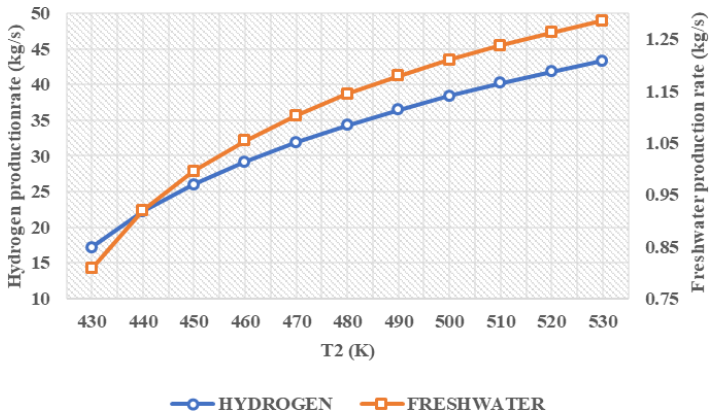

Fig. 5. The effect of collector outlet temperature on the value of hydrogen and freshwater production rates.

water production rates. The five working fluids analyzed include n-pentane, R245fa, R134a, Isobutane, and R600. The results show that R600 yields the highest production rates for both hydrogen and freshwater among the fluids tested. This increased performance is attributed to the higher energy output generated by the ORC cycle when utilizing R600 as the working fluid.

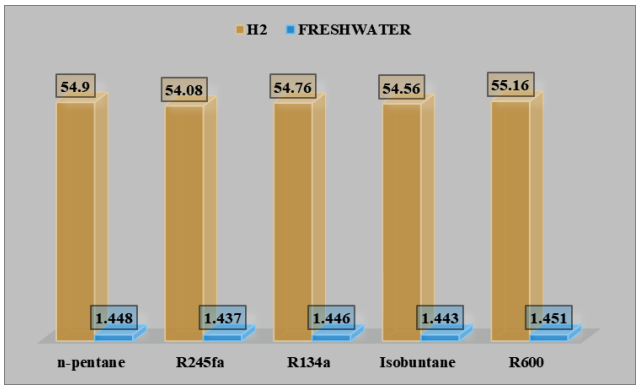

Fig. 6. Evaluation of five distinct working fluids regarding their rates of hydrogen and freshwater production.

4 Conclusion

The research develops a multigeneration platform which produces electricity, hydrogen, and freshwater, while also providing heating and cooling solutions to meet the growing demand for integrated sustainable energy technologies. The Evacuated Tube Collector (ETC) serves as the primary thermal energy source by heating the geothermal fluid. The integrated system comprises several essential subsystems, including an Organic Rankine Cycle (ORC) for electricity generation, a double-effect absorption refrigeration system for cooling, a domestic water heater for thermal needs, PEM electrolyzers for hydrogen production, and reverse osmosis (RO) desalination units for freshwater management. The results indicate that increasing the energy input into the collector system not only raises its outlet temperature but also enhances the overall power generation capability of the system. The collector operates at maximum efficiency in both energy performance and exergy efficiency when solar intensity rates are higher, resulting in improved performance across all subsystems. The production rates of both hydrogen and freshwater increase as the outlet temperature of the collector rises, as thermal conditions have a significant impact on these output values. The analysis revealed that R600 outperforms the other tested substances due to its superior thermodynamic properties for hydrogen and freshwater production. The research indicates that R600 holds great potential for use in future multigeneration systems. Overall, the proposed system positions itself as an effective solution for optimizing renewable energy resources by integrating multiple energy services into a single, cohesive system.

References

[1] Holechek JL, Geli HM, Sawalhah MN, Valdez R. A global assessment: can renewable energy replace fossil fuels by 2050? Sustainability. 2022;14(8):4792.

[2] Zastempowski M. Analysis and modeling of innovation factors to replace fossil fuels with renewable energy sources-Evidence from European Union enterprises. Renewable and Sustainable Energy Reviews. 2023;178:113262.

[3] Ishaq H, Dincer I. Comparative assessment of renewable energy-based hydrogen production meth-

ods. Renewable and Sustainable Energy Reviews. 2021;135:110192.

[4] Bischi A, Taccari L, Martelli E, Amaldi E, Manzolini G, Silva P, et al. A detailed MILP optimization model for combined cooling, heat and power system operation planning. Energy. 2014;74:12-26.

[5] Mokhtari A, Haqiqati A. Energy, Economic and Environmental Multi-objective Optimization of a Novel Hybrid Solar-geothermal Power Generation Using Organic Rankine Cycle for Off-Grid Application with Energy Storage. Iranica Journal of Energy & Environment. 2025;16(3):426-38.

[6] Forghani AH, Solghar AA, Hajabdollahi H. Optimal design of a multi-generation system based on solar and geothermal energy integrated with multi-effect distillatory. Applied Thermal Engineering. 2024;236:121381.

[7] Ren F, Wei Z, Zhai X. Multi-objective optimization and evaluation of hybrid CCHP systems for different building types. Energy. 2021;215:119096.

[8] Alirahmi SM, Dabbagh SR, Ahmadi P, Wongwises S. Multi-objective design optimization of a multi-generation energy system based on geothermal and solar energy. Energy Conversion and Management. 2020;205:112426.

[9] Zarei A, Akhavan S, Ghodrat M, Behnia M. Thermodynamic analysis and multi-objective optimization of a modified solar trigeneration system for cooling, heating and power using photovoltaic-thermal and flat plate collectors. International Communications in Heat and Mass Transfer. 2022;137:106261.

[10] Calise F, Cappiello FL, Dentice d'Accadia M, Vicidomini M. Thermo-economic analysis of hybrid solar-geothermal polygeneration plants in different configurations. Energies. 2020;13(9):2391.

[11] Yilmaz C, Sen O. Feasibility of optimum energy use and cost analyses by applying artificial intelligence and genetic optimization methods in geothermal and solar energy-assisted multigeneration systems. Renewable Energy. 2024;237:121548.

[12] Budihardjo I, Morrison GL. Performance of water-in-glass evacuated tube solar water heaters. Solar Energy. 2009;83(1):49-56.